Effects of barium, lanthanum and gadolinium on endogenous chloride and potassium currents in *Xenopus* oocytes

T. Tokimasa *† and R. A. North

*Glaxo Institute for Molecular Biology, 14 chemin des Aulx, Plan-les-Ouates 1228, Geneva, Switzerland and *Department of Physiology, Kurume University School of Medicine, Kurume 830, Japan*

1. The effects of multivalent cations on membrane currents recorded from *Xenopus* oocytes were studied.

2. The hyperpolarization-activated chloride current was reversibly blocked by lanthanum; half-maximal block occurred at a concentration of 8 μM. Zinc, cadmium, cobalt and nickel were less potent than lanthanum, and gadolinium, manganese, barium and strontium had no effect at a concentration of 100 μM.

3. The calcium-activated chloride current was blocked by gadolinium (50 μM), and lanthanum, cadmium, cobalt, nickel and manganese were equally effective. The actions of gadolinium and lanthanum were almost irreversible, while partial (30–80%) recovery was observed with the other cations. Zinc (100 μM) had no effect.

4. In lanthanum (100 μM), membrane depolarizations from −70 mV activated an outward potassium current that was partially blocked by barium (0·1–2 mM). The barium-sensitive current was confined to potentials less negative than −70 mV. The current consisted of a time-independent as well as a time-dependent component, the latter of which had voltage dependence similar to the M-current.

5. It is proposed that lanthanum, gadolinium and barium can usefully separate these endogenous membrane currents in *Xenopus* oocytes.

Oocytes of *Xenopus laevis* have been widely used for cloning and heterologous expression of ion channels (see Jentsch, 1994), but the results can be complicated by the existence of ionic currents endogenous to oocytes (see Pusch & Jentsch, 1994). For example, the inwardly rectifying potassium channel was cloned by functional expression in oocytes, although some batches of eggs clearly have a similar endogenous current (Kubo, Baldwin, Jan & Jan, 1993). Furthermore, it is common in such experiments to wait several days after injection of the foreign RNA, and it is therefore important to know whether the expression of endogenous currents changes with time after removal of oocytes from the ovary. The purpose of the present experiments was to isolate three endogenous currents and determine whether they could be eliminated selectively by multivalent cations. The currents studied have been reported previously, although not all have been fully characterized. They were the hyperpolarization-activated chloride current (Peres & Bernardini, 1983; Chesnoy-Marchais, 1983; Parker & Miledi, 1988; Kowdley, Ackerman, John, Jones & Moorman, 1994), the calcium-activated chloride current (Barish, 1983) and the voltage-dependent potassium current (Taglietti, Tanzi, Romero & Simoncini, 1984; Peres, Bernardini, Mancinelli & Ferroni, 1985).

METHODS

Xenopus laevis were anaesthetized with MS-222 (3-aminobenzoic acid ethyl ester methanesulphonate salt, 0·4%) and decapitated. A lobule of ovary was dissected free, and theca and follicular cells were removed by incubation in a solution containing (mM): NaCl, 82·5; KCl, 2·5; $NaHPO_4$, 1; Hepes, 5 (pH adjusted to 7·6 with NaOH); and collagenase (2 mg ml^{-1}; Type 1A, Sigma). The oocytes were stored at 18 °C for 1–10 days in a Ringer solution of the following composition (mM): NaCl, 96; KCl, 2; $CaCl_2$, 1·8; $MgCl_2$, 1; sodium pyruvate, 5; Hepes, 5 (pH adjusted to 7·5 with NaOH); and penicillin (10 units ml^{-1}) and streptomycin (10 μg ml^{-1}). This solution, but without antibiotics, was also used for electrophysiological recordings; individual oocytes were continuously superfused at 4–10 ml min^{-1}. In some experiments the pH of the solution was brought to 6·5 or 8·5 by addition of HCl or NaOH.

Two microelectrodes were inserted into the oocyte; they contained potassium chloride (3 M) and had resistances from 0·6 to 1·2 MΩ.

† To whom correspondence should be addressed at the Department of Physiology, Tokai University School of Medicine, Bohseidai, Isehara 259-11, Japan.

The reference electrode was a Ag–AgCl wire in an agar–KCl bridge; the potential at this electrode changed by 1·8 ± 0·3 mV ($n = 4$) when the chloride concentration in the solution was reduced to 10 mM (substitution with isethionate); however, this was not taken into account. Recordings were made on the day of the dissociation (defined as day 1) as well as on the following 2–10 days. In the first four batches of oocytes examined, the resting membrane potential ranged from −42 to −89 mV (−65·1 ± 0·8 mV, mean ± S.E.M.; $n = 148$) during days 1–6. The standard deviation of the mean was 9·8 mV. In all subsequent experiments (batches 5–29) we used only those oocytes that had a resting membrane potential between −55 and −75 mV.

Membrane potential and membrane currents were controlled and recorded using an Axoclamp-2B amplifier and pCLAMP software (version 5.71; Axon Instruments); Axograph (version 1.1; Axon Instruments) was used for off-line analysis. Steady-state conductances (G) were calculated by dividing current by driving force, and were normalized to their maximal values (G_{max}). A least-squares method was used to fit G/G_{max} to voltage (V) according to the Boltzmann expression:

$$G/G_{max} = \{1 + \exp((V_{0.5} - V)/k)\}^{-1},$$

where $V_{0.5}$ is the membrane potential at half-maximal inactivation and k is the slope factor. Experiments were carried out at room temperature (22–24 °C). Numerical values are presented as means ± S.E.M. for the number of cells tested (n). Differences were considered to be significant if $P < 0.05$ using Student's paired or unpaired t test. Drugs used were 4-aminopyridine (4-AP), sodium isethionate, (±)-muscarine chloride and tetraethylammonium chloride (TEA; all from Sigma).

A proportion of oocytes showed spontaneous inward chloride currents (Kusano, Miledi & Stinnakre, 1982) when voltage clamped at −60 mV (range, 10–1000 nA); this proportion was less than 10% in twelve batches between July and mid-September but more than 70% in seventeen batches tested from mid-September to November. Cells showing this chloride current have not been used in the present study. Muscarine (20 μM) was used to evoke a chloride current in fourteen oocytes; this current (110 ± 36 nA at −55 mV) reversed polarity from inward to outward at −18·0 ± 0·9 mV, as measured by intersection of the current–voltage (I–V) plots (2 s ramp from −75 to +25 mV). From this we estimated the intracellular chloride concentration under the present circumstances to be 56 mM (Kusano *et al.* 1982).

RESULTS

Chloride currents

Figure 1*A* shows typical recordings of membrane currents obtained from one oocyte on the day of its dissociation (day 1); the membrane potential (holding potential, −60 mV) was changed in a stepwise manner to ten different test potentials for 3 s. Two chloride currents were readily distinguished. One was the calcium-activated chloride current ($I_{Cl,Ca}$), which was transiently activated by strong depolarizing steps (Barish, 1983); the other was the larger hyperpolarization-activated chloride current ($I_{Cl,h}$) (Parker & Miledi, 1988; Moorman, Palmer, John, Durieux & Jones, 1992; Kowdley *et al.* 1994). $I_{Cl,h}$ was responsible for the very pronounced inward rectification in the steady-state I–V plot (Fig. 1*B*); the amplitudes and other properties of these currents were very similar to the previous descriptions.

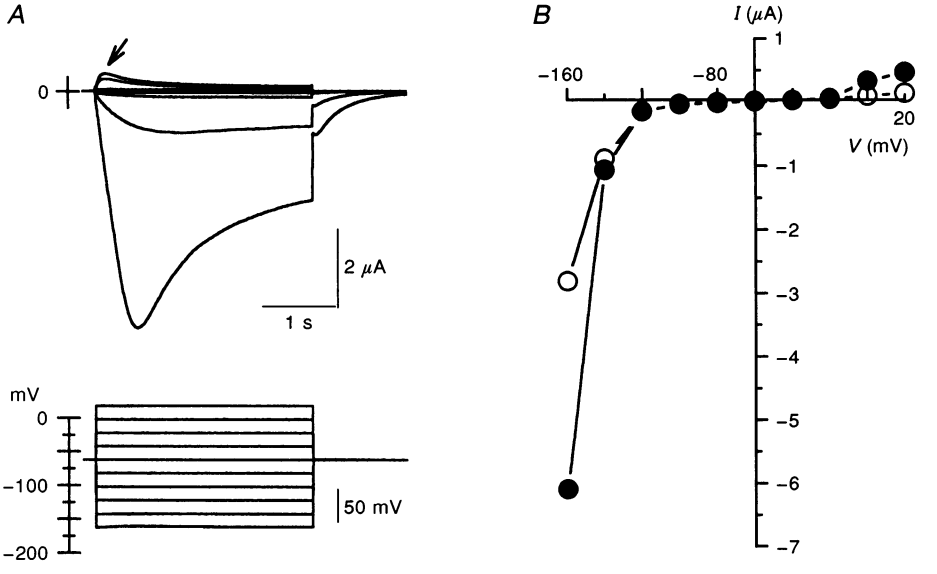

Figure 1. Membrane currents in *Xenopus* oocytes

Results from 1 oocyte (day 1) with the holding potential at −60 mV. The membrane potential was changed for 3 s to test potentials from +20 to −160 mV in −20 mV increments. *A*, superimposed current traces (upper panel) and command pulses (lower panel). The activating $I_{Cl,h}$ is followed by the deactivating tail current after the termination of the command pulses. The arrow indicates the outward peak at +20 mV, which is largely activation of $I_{Cl,Ca}$. *B*, I–V relationship of this oocyte measured at the end of the pulses (○) and from the inward (or outward) peak during the pulses (●). In this and other figures, the zero current level is indicated on the left-hand side of the baseline for each family of current traces.

$I_{Cl,Ca}$ averaged 224 ± 20 nA (range, 50–420 nA; $n = 32$) in response to step depolarizations from −60 to +20 mV; the amplitude was approximately doubled with steps from −120 mV, and the voltage at half-maximal steady-state inactivation was −62·1 ± 1·9 mV (slope factor of 17·1 ± 2·3 mV; $n = 7$). This current was eliminated in a calcium-free solution ($n = 3$) or by addition of gadolinium (50 μM; $n = 6$; Fig. 2*A* and *B*); gadolinium was quite useful for measuring the reversal potential of $I_{Cl,h}$ in the absence of $I_{Cl,Ca}$ (Fig. 2*C* and *D*; see below). Lanthanum (50 μM; $n = 6$), cadmium (50 μM; $n = 6$), cobalt (50 μM; $n = 6$), nickel (50 μM; $n = 2$) and manganese (50 μM; $n = 1$) were as effective as lanthanum. The actions of lanthanum and gadolinium were almost irreversible, whereas partial (30–80%) recovery was observed with the other cations. Zinc (50–100 μM; $n = 5$) had no effect.

Lanthanum (0·1–300 μM) reversibly inhibited $I_{Cl,h}$ (Fig. 3*A* and *B*) with a half-maximal concentration of about 8 μM (Fig. 3*C*; see also Discussion). In contrast, gadolinium (100 μM) inhibited $I_{Cl,h}$ by 3 ± 1% (range, 0–9%) in six cells in which lanthanum (100 μM) inhibited $I_{Cl,h}$ by 91·3 ± 1·7% (range, 89–95%). At this concentration, the inhibition by other cations was 56·3 ± 4·1% for zinc ($n = 5$), 37·2 ± 1·5% for cadmium ($n = 4$), 33·8 ± 5·6% for cobalt ($n = 3$) and 6·5 ± 4·2% for nickel ($n = 3$); manganese ($n = 3$), barium ($n = 6$) and strontium ($n = 3$) had no effect. The reversal potential of $I_{Cl,h}$ could be measured in the presence of gadolinium (100 μM) and the values were −18·3 ± 1·0 mV ($n = 34$), 0·4 ± 1·8 mV ($n = 10$) and 39·2 ± 4·8 mV ($n = 4$) when the concentration of chloride ions in the superfusate was 103·6, 50 and 10 mM, respectively (Fig. 2*C* and *D*).

We noticed that the amplitude of $I_{Cl,h}$ (recorded at −140 mV) was dependent on the number of days after removal of the oocytes. It was largest on day 1, declined to a minimum on days 3 and 4 and became somewhat larger again on days 5

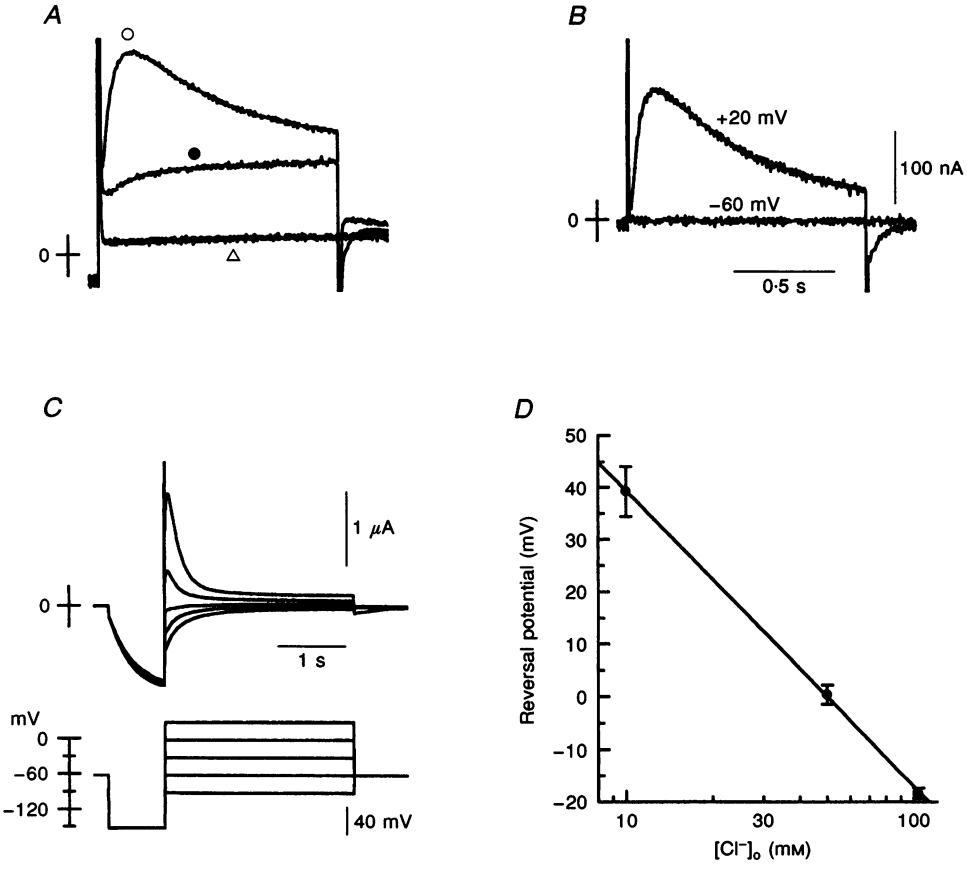

Figure 2. Isolation of $I_{Cl,h}$ by gadolinium

A and *B*, results from 1 oocyte (day 6) with the holding potential at −60 mV. $I_{Cl,Ca}$ was activated at +20 mV (voltage trace not shown) following the prepulse (to remove the inactivation) from −60 to −120 mV for 2 s. *A*: ○, control; ●, gadolinium (50 μM); △, ohmic current upon steps to −60 mV in control and in gadolinium. *B*, $I_{Cl,Ca}$ (gadolinium-sensitive current) in *A* at +20 mV. *C*, superimposed current traces (upper panel) and command pulses (lower panel) in the presence of gadolinium (100 μM); results from the same cell as that in Fig. 1. *D*, semilogarithmic plots of the reversal potential of $I_{Cl,h}$ in gadolinium (100 μM).

and 6; in contrast, $I_{Cl,Ca}$ showed little change over six days (Fig. 4*A*). However, even at day 3 a large $I_{Cl,h}$ could be elicited if the hyperpolarization was further increased (Fig. 4*B*). This implies that the voltage dependence of the current changes rather than the number of channels. Figure 4*C* shows conductance–voltage ($G-V$) plots for the same batch of oocytes tested at days 1, 4, 5 and 6. It is clear that the time-dependent changes in $I_{Cl,h}$ can be explained, at least in part, by changes in its voltage dependence. $I_{Cl,h}$ was strongly pH dependent (Fig. 4*D* and *E*). In sixteen cells (day 2) it was observed that the mid-point for activation of $I_{Cl,h}$ was depolarized by 10–15 mV by a tenfold reduction in proton concentration (pH 8·5) and hyperpolarized by 15–20 mV by a tenfold increase in proton concentration (pH 6·5); these effects were fully reversible.

Potassium currents

Figure 5 shows that barium (1 mM) caused a 35 mV depolarization which was associated with an increase in the amplitude of the hyperpolarizing electrotonic potentials. The actions of barium (10 μM to 1 mM) were concentration dependent. Among three cells, the peak amplitude of the depolarization was 28·3 ± 3·4, 16·3 ± 3·2 and 4·2 ± 1·3 mV with a concentration of barium in the superfusate of 1 mM, 100 μM and 10 μM, respectively. Barium (1 μM) had no effect in these cells. In seven other cells, the peak amplitude of the depolarization caused by barium (1 mM) was 28·4 ± 2·5 mV even when measured in the presence of lanthanum (100 μM). TEA (16–48 mM), 4-AP (1–3 mM) and caesium (2 mM) did not mimic the action of barium ($n = 3$; Fig. 5; 4-AP and caesium data not shown in Fig. 5). These observations suggest that there is an on-going barium-sensitive outward current near the resting membrane potential; the properties of this were examined under voltage clamp in the presence of lanthanum (100 μM).

Oocytes were subjected to depolarizing ramp (20 mV s^{-1}) commands from −120 to +60 mV (basic holding potential,

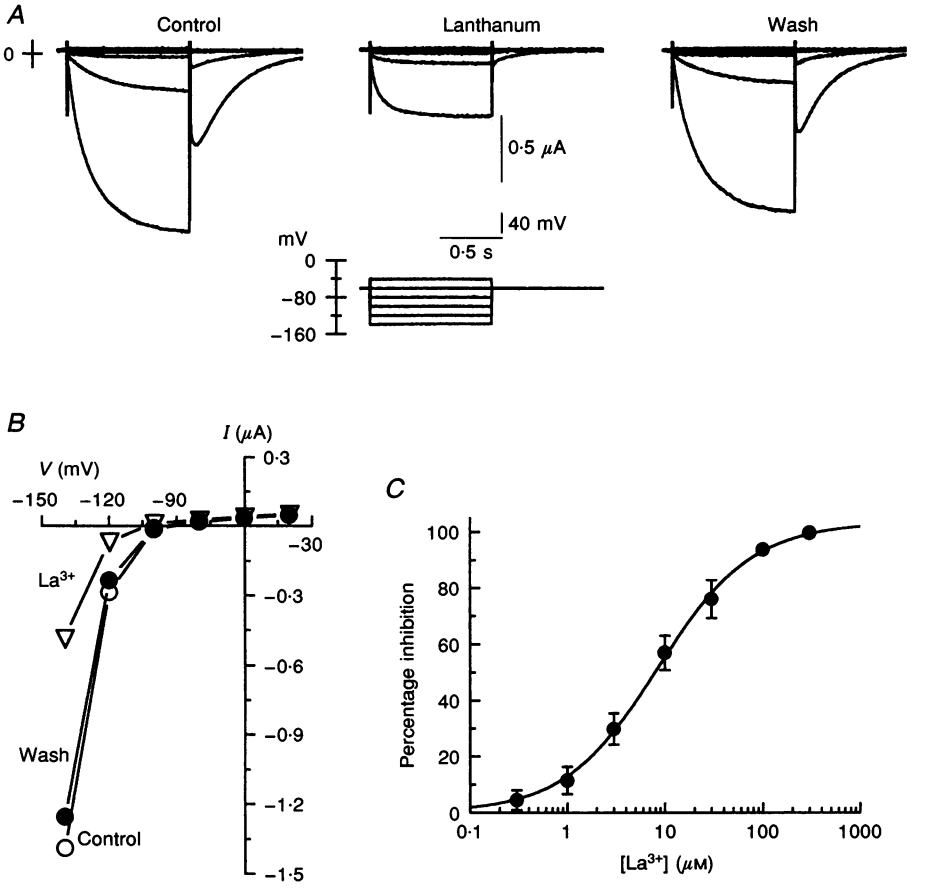

Figure 3. Lanthanum inhibits $I_{Cl,h}$

A, reversible inhibition of $I_{Cl,h}$ by lanthanum (10 μM). Holding potential was −60 mV; test potentials from −40 to −140 mV in −20 mV increments. *B*, $I-V$ relationship for the results in *A*; ○, control; ▽, lanthanum; ●, wash. *C*, dose–response curve for the inhibition of $I_{Cl,h}$ by lanthanum. Points are means ± S.E.M. ($n = 26$ for 100 μM and 4–7 for other concentrations). Line is least-squares fit to: inhibition = $100[La]^n/([La]^n + IC_{50}{}^n)$, where [La] is the lanthanum concentration; the Hill coefficient, n, is 0·9; and the IC_{50} is 8 μM.

−60 mV; Fig. 6). Barium (2 mM) inhibited outward rectification in the $I-V$ curve without affecting a current component between −70 and −120 mV. The amplitude of the barium-sensitive current ranged from 25 to 65 nA at +10 mV and fell off to zero between −59 and −75 mV (−70·6 ± 1·3 mV; $n = 13$).

In the next series of experiments, oocytes were subjected to depolarizing pulse commands (5–100 mV, 1–3 s) from a holding potential of −70 mV and the barium-sensitive current was defined by subtracting the currents after applying 2 mM barium (Fig. 7*A* and *B*). The barium-sensitive current had a time-independent (or otherwise very fast) as well as a time-dependent slow component; the latter caused the deactivating tail current upon stepping back from test potentials to the holding potential of −70 mV (Fig. 7*A*). Among nine cells, the fraction of the tail current was related to membrane potential by a Boltzmann expression with a $V_{0.5}$ value of −23 mV and a k value of 13 mV (Fig. 7*C*).

The $I-V$ relationship for the barium-sensitive current (e.g. Fig. 7*B*) could be described by:

$$I = (V - E)G_{max}\{1 + \exp((V_{0.5} - V)/k)\}^{-1},$$

where E is the reversal potential of the current (see below), and the remaining part of the equation represents the Boltzmann expression (see Methods); E was assumed to be −97 mV (see Fig. 8*C*) for both the time-independent and time-dependent components. The data points were fitted to the equation (least-squares method) giving a $V_{0.5}$ value of −31·9 ± 2·1 mV ($n = 9$);

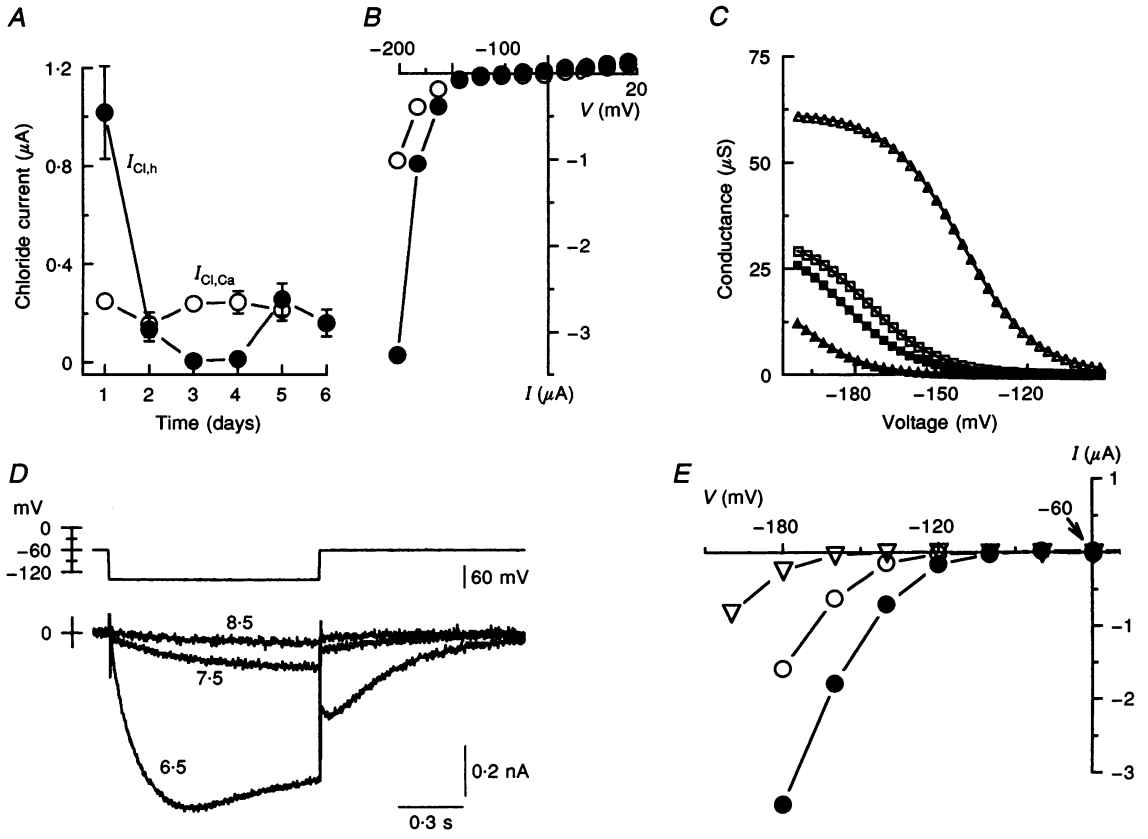

Figure 4. Time and pH dependence of $I_{Cl,h}$

A–C, amplitude of $I_{Cl,h}$ measured at different times after oocyte removal. *A*: ●, $I_{Cl,h}$, measured at −140 mV; ○, $I_{Cl,Ca}$, measured at +20 mV. Results pooled from 4 batches of oocytes. For days 1–6, respectively, $n = 47$, 30, 17, 30, 19 and 21 for $I_{Cl,h}$ and 8, 7, 5, 8, 4 and 0 for $I_{Cl,Ca}$. *B*, $I-V$ plots obtained from 2 oocytes; ○, day 3; ●, day 5. *C*, $G-V$ relationship for 1 batch of oocytes ($n = 23$) examined on different days. Means of 5–7 oocytes; for clarity S.E.M. values have been omitted. Continuous lines are Boltzmann fits (see text). △, day 1 oocytes: $V_{0.5}$, −143 ± 9·1 mV; k, 12·9 ± 1·9 mV; G_{max}, 61·7 ± 20·2 μS ($n = 6$). ▲, day 4 oocytes: $V_{0.5}$, −199 ± 6·1 mV; k, 11·1 ± 1·2 mV; G_{max}, 23·7 ± 11·3 μS ($n = 7$). □, day 5 oocytes: $V_{0.5}$, −175 ± 6·1 mV; k, 12·2 ± 1·5 mV; G_{max}, 33·1 ± 9·9 μS ($n = 5$). ■, day 6 oocytes: $V_{0.5}$, −183 ± 7·1 mV; k, 12·1 ± 1·5 mV; G_{max}, 32·1 ± 6·1 μS ($n = 5$). *D* and *E*, sensitivity of $I_{Cl,h}$ to protons. *D*, results obtained from a single oocyte (day 2) in response to hyperpolarizing step commands (80 mV, 1 s) from the holding potential of −60 mV. The pH is indicated beside each current response. *E*, $I-V$ plots for the inward peak of $I_{Cl,h}$. ▽, pH 6·5; ○, pH 7·5; ●, pH 8·5.

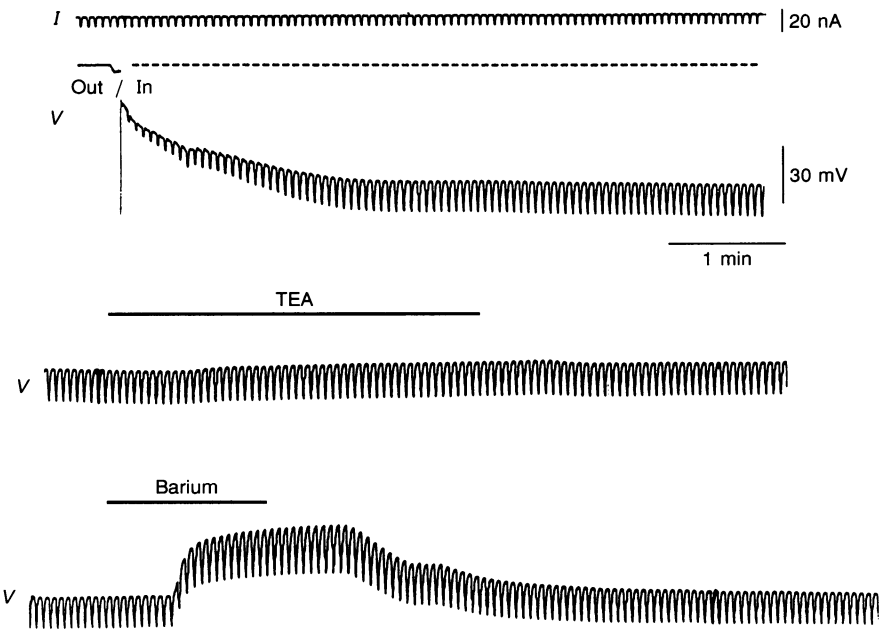

Figure 5. Barium-induced depolarization

Results from 1 oocyte on day 3; the 3 voltage traces (indicated by *V*) are continuous and show the membrane potential during the period after impaling the oocyte with two microelectrodes (dashed line). Constant current pulses (8 nA, 1 s, indicated by *I*) were passed at 0·25 Hz; current traces are not shown for the results with TEA and barium. Membrane potential was unaffected by TEA (48 mM) but was much reduced by barium (1 mM). At the onset of the barium application the membrane potential was −65 mV and the input resistance was 2·1 MΩ.

other parameters were 12·4 ± 0·4 mV for k and 411 ± 41·2 nS for G_{max}. This implies that the $V_{0.5}$ value for the time-independent component is slightly more negative than that of the time-dependent component.

The barium-sensitive current could be activated continuously by setting the holding potential at 0 mV, then deactivated briefly (2 s) during hyperpolarizing step commands (Fig. 8*A*). The holding current at 0 mV showed little change over 50–70 s recording time (Fig. 8*A*) indicating that the barium-sensitive current is non-inactivating. The polarity of the tail current (e.g. outward at −70 mV) reversed at about −95 and −40 mV with a concentration of potassium ions in the superfusate of 2 and 20 mM, respectively (Fig. 8*B*

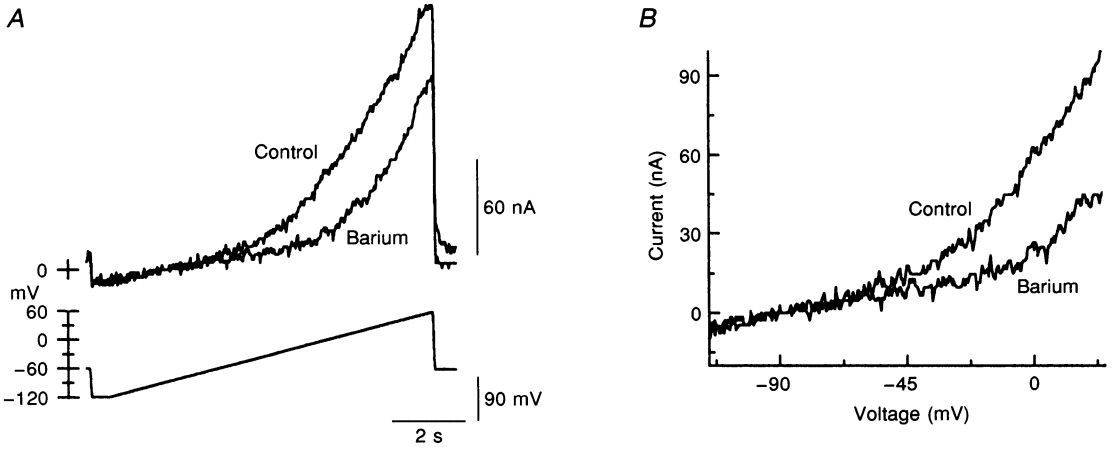

Figure 6. Voltage dependence of barium-sensitive current in the *I–V* curve

A, results obtained from a single cell. The cell membrane was hyperpolarized in a stepwise manner from −60 to −120 mV, then slowly (20 mV s^{-1}) depolarized to +60 mV using the ramp command (lower panel). The control response and that in the presence of barium (2 mM) are superimposed. *B*, *I–V* plots obtained from the records in *A*.

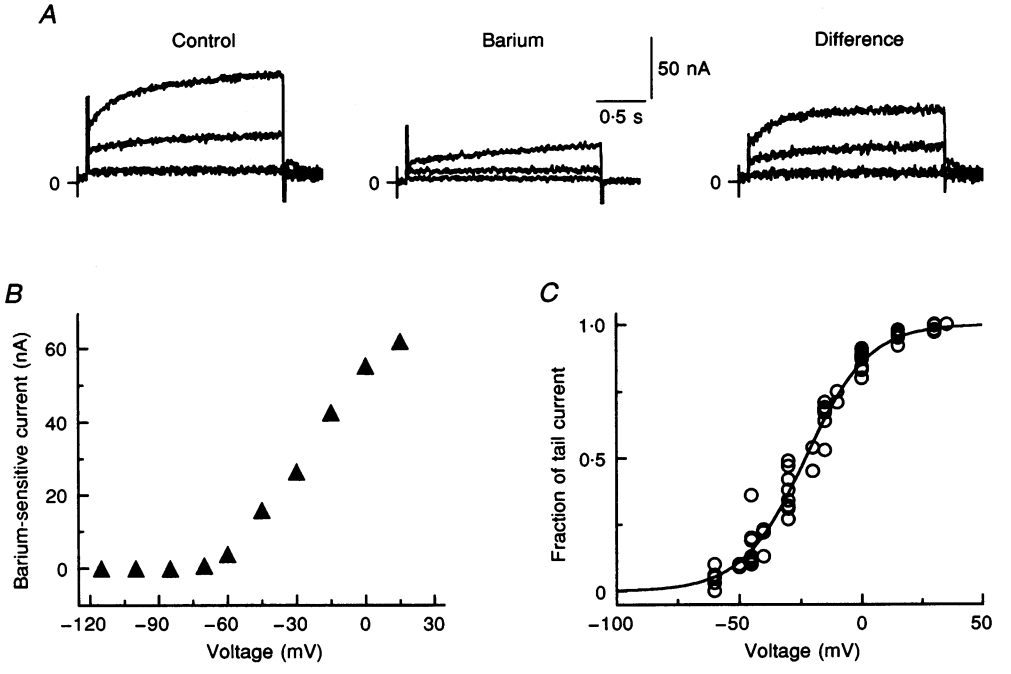

Figure 7. Voltage dependence of barium-sensitive outward current

Results in *A* and *B* were obtained from a single oocyte. *A*, currents evoked by depolarization from −70 mV to −60, −30 and 0 mV, before (left) and during (middle) application of barium (2 mM). The barium-sensitive difference current is shown on the right. *B*, *I–V* plot for the barium-sensitive current of the cell in *A*. Note that the barium-sensitive current is non-existent at potentials negative to −70 mV (see Fig. 6). *C*, fraction of barium-sensitive tail current at −70 mV, after stepping back from the potential indicated. Data from 9 oocytes. The continuous line is the least-squares fit to a Boltzmann function; $V_{0.5}$ is −23·3 mV and k is 13 mV.

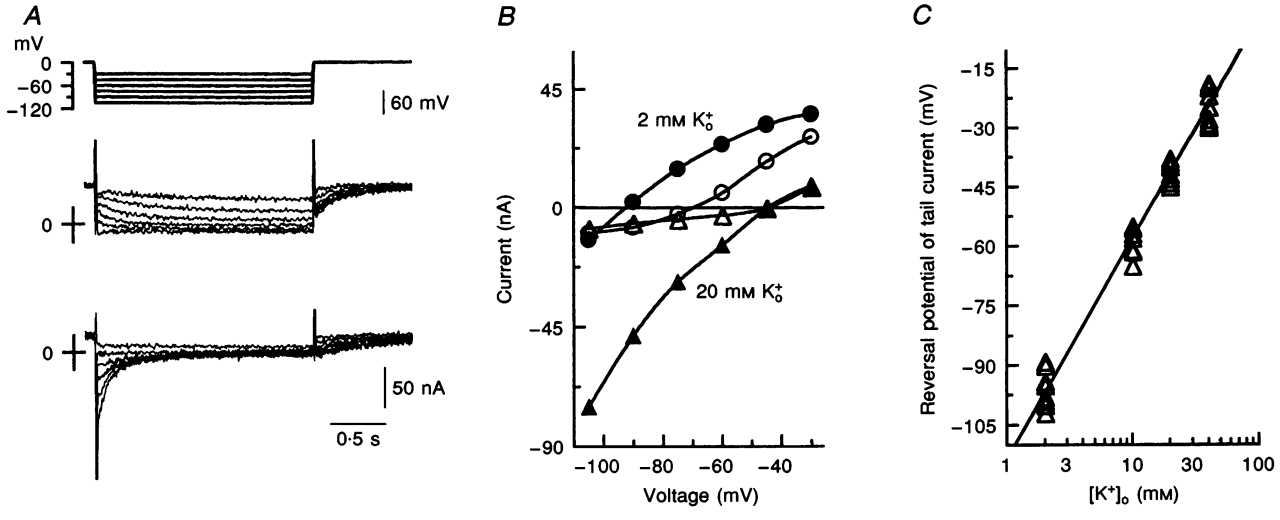

Figure 8. Barium-sensitive outward current is potassium selective

Results in *A* and *B* were obtained from a single oocyte. *A*, superimposed command pulses (top) indicate that the barium-sensitive current was continuously activated at 0 mV, then briefly deactivated during hyperpolarizing step commands. Superimposed current traces (middle and bottom) were obtained in 2 and 20 mM potassium, respectively. Lanthanum (100 μM) and caesium (2 mM) were present. *B*, *I–V* plots for the records in *A*; circles, 2 mM K_o^+; triangles, 20 mM K_o^+; filled symbols, instantaneous plots; open symbols, steady-state plots measured at the end of command pulses. *C*, reversal potential of the tail current is linearly related to the log of the extracellular potassium concentration. The slope of the regression line is 55·4 mV per decade.

and C). Among cells, the reversal potential of the tail current was $-96{\cdot}8 \pm 1{\cdot}5$ ($n = 10$), $-58{\cdot}5 \pm 1{\cdot}3$ ($n = 8$), $-41{\cdot}6 \pm 0{\cdot}8$ ($n = 10$) and $-24{\cdot}7 \pm 1{\cdot}5$ mV ($n = 9$) when measured in 2, 10, 20 and 40 mM potassium, respectively (Fig. 8C). The regression of reversal potential on potassium concentration had a slope of 55·4 mV per decade. Figure 8B also shows that the instantaneous I–V plot for the barium-sensitive current (activated at 0 mV) intersected with the zero current line between −40 and −45 mV in the potassium-rich (20 mM) solution. This implies that the time-independent component is also carried by potassium ions.

Activation and deactivation of the time-dependent component were exponential functions of time at all voltages tested (Fig. 9A–C). The time constant (τ) was measured at a range of membrane potentials and fitted by least squares to $\tau = (\alpha + \beta)^{-1}$ where:

$$\alpha = \alpha_0 \exp((zF/2RT)(V - V_{0.5}))$$

and

$$\beta = \beta_0 \exp((-zF/2RT)(V - V_{0.5})),$$

where F is Faraday's constant, R is the universal gas constant, and T is absolute temperature. This provided estimates (Fig. 9D) of −27 mV for $V_{0.5}$ (when $\alpha = \alpha_0 = \beta = \beta_0 = 0{\cdot}85\ s^{-1}$) and 1·7 for for the valency z; this kinetic estimate of $V_{0.5}$ agrees well with the steady-state estimates obtained from the tail currents.

Barium (2 mM) did not completely block the endogenous voltage-dependent potassium current. In the presence of barium (and lanthanum), the residual current activated by depolarization had essentially the same properties as the barium-sensitive component, or more precisely the time-dependent component to the barium-sensitive potassium current described above.

DISCUSSION

The two main conclusions of the present work are that the two endogenous chloride currents $I_{Cl,h}$ and $I_{Cl,Ca}$ can be readily distinguished (both by gadolinium block and by their distinct dependence on the time after oocyte removal), and that oocytes have a previously uncharacterized, barium-sensitive, voltage-dependent potassium current.

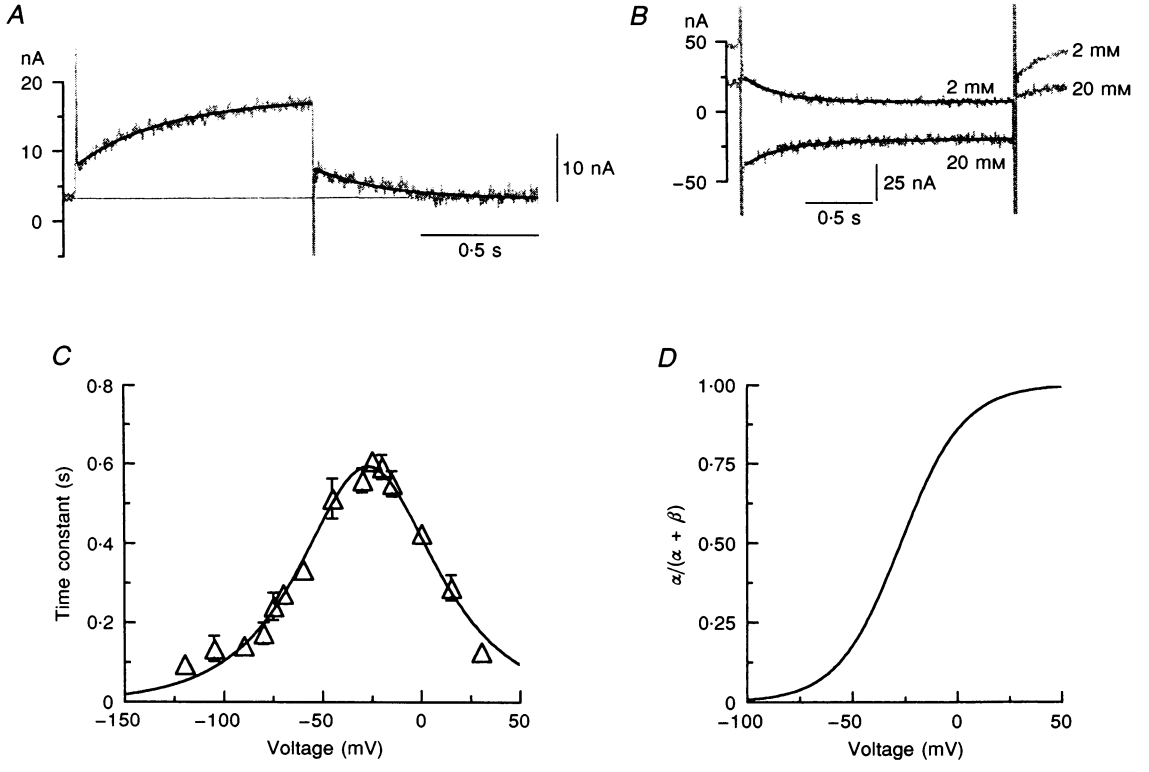

Figure 9. Kinetics of time-dependent component of the barium-sensitive potassium current

A, activation at −50 mV (time constant, 370 ms) followed by deactivation at −70 mV (time constant, 293 ms). Continuous lines are single exponential fits. B, deactivating tail currents at −60 mV in 2 and 20 mM potassium (time constant, 265 ms in both cases). C, dependence of time constant on potential. Each data point was obtained from 3–55 measurements from more than 20 oocytes; from −120 to −50 mV data are time constants of deactivation; from −20 to +30 mV data are time constants of activation; and data at −45 to −30 mV contain both the activation and deactivation time constants. Experiments in 2–40 mM potassium. Continuous line is least-squares fit to $\tau = (\alpha + \beta)^{-1}$, where $\alpha = \alpha_0 \exp((zF/2RT)(V - V_{0.5}))$ and $\beta = \beta_0 \exp((-zF/2RT)(V - V_{0.5}))$ (see text). D, plot for $\alpha/(\alpha + \beta)$ as a function of voltage.

Parker & Miledi (1988) reported that only a limited number of oocytes display $I_{Cl,h}$ and that even when present the current simply disappears within a few days after the removal of oocytes from the ovary. In contrast, Kowdley *et al.* (1994) reported that the magnitude of the current (their $I_{Cl(endo)}$) does not show time-dependent changes, but that it varied considerably among batches of eggs. The present study indicates that the underlying channels are present in all eggs, and that the time-dependent changes result, at least in part, from shifts in voltage sensitivity (Fig. 4*A–C*). There are other differences between the present results and those of Kowdley *et al.* (1994). We found that 100 μM barium had no effect, whereas they found about 40% block of the current at −160 mV; we found a shift in voltage dependence of 10–15 mV per tenfold shift in proton concentration, whereas they reported no such effects. The explanation for these differences is not obvious; we only used enzymatically defolliculated oocytes with resting potentials close to −65 mV (2 mM external potassium), whereas Kowdley *et al.* (1994) used manually defolliculated eggs held at −10 mV. The proton dependence that we have observed suggests that pH dependence might not be a reliable criterion to distinguish the endogenous channels from those expressed by injection of phospholemman RNA (Moorman *et al.* 1992). In any event, the present work suggests that both endogenous chloride currents can be eliminated by 100 μM lanthanum, whereas the same concentration of gadolinium selectively blocks the calcium-activated current.

Regarding the actions of multivalent cations on $I_{Cl,h}$, we noticed that the cations used (including zinc) inhibited the deactivating tail current more severely than the activating current (e.g. Fig. 3*A*). It is unlikely that the observations are due to contamination by the activating $I_{Cl,Ca}$ at −60 mV, for two main reasons. First, −60 mV was too negative to observe the activating $I_{Cl,Ca}$. Second, zinc had no effect on $I_{Cl,Ca}$. In many cells, $I_{Cl,h}$, which was non-inactivating in the control, now showed marked inactivation in zinc (data not shown). Lanthanum and other cations had similar (though weaker) actions to those of zinc. Since our main goal in the present study was to find cations (e.g. lanthanum) which can isolate potassium currents from chloride currents, we simply measured the amplitude of $I_{Cl,h}$ at the end of the hyperpolarizing command pulses instead of measuring the amplitude of the tail current. It is therefore obvious that further experiments are necessary to characterize more fully the actions of cations (zinc in particular) on $I_{Cl,h}$.

The endogenous voltage-dependent potassium current may complicate experiments in which exogenous channels are expressed, although this is likely to be a problem only with poorly expressing RNAs. The amplitude of the endogenous barium-sensitive potassium current was typically several tens of nanoamperes. Barium blocks most voltage-dependent potassium currents, so this property is not likely to be useful in the separation of exogenous and endogenous currents. A more useful distinguishing feature may be the kinetics of activation and deactivation; these are considerably slower than those seen for heterologously expressed potassium channels in the K_v series (Stuhmer *et al.* 1989) although similar to the values seen for the duplicated pore motif potassium channel of yeast (Reid *et al.* 1996). However, although the endogenous current may be small in amplitude relative to the currents observed with heterologous expression, the powerful depolarizing effect of barium indicates that it is an important contributor to the resting potential of the oocyte. Small changes in the level of expression of this current could have a large effect on the resting potential of the oocyte. The residual potassium current that is largely insensitive to barium probably corresponds to that described by Parker & Ivorra (1990).

Barish, M. E. (1983). A transient calcium-dependent chloride current in the immature *Xenopus* oocyte. *Journal of Physiology* **342**, 309–325.

Chesnoy-Marchais, D. (1983). Characterization of a chloride conductance activated by hyperpolarization in *Aplysia* neurones. *Journal of Physiology* **342**, 277–308.

Jentsch, T. J. (1994). Molecular physiology of anion channels. *Current Opinion in Cell Biology* **6**, 600–606.

Kowdley, G. C., Ackerman, S. J., John, J. E. III, Jones, L. R. & Moorman, J. R. (1994). Hyperpolarization-activated chloride currents in *Xenopus* oocytes. *Journal of General Physiology* **103**, 217–230.

Kubo, Y., Baldwin, T. J., Jan, Y. N. & Jan, L. Y. (1993). Primary structure and functional expression of a mouse inward rectifier potassium channel. *Nature* **362**, 127–133.

Kusano, K., Miledi, R. & Stinnakre, J. (1982). Cholinergic and catecholaminergic receptors in the *Xenopus* oocyte membrane. *Journal of Physiology* **328**, 143–170.

Moorman, J. R., Palmer, C. J., John, J. E., Durieux, M. E. & Jones, L. R. (1992). Phospholemman expression induces a hyperpolarization-activated chloride current in *Xenopus* oocytes. *Journal of Biological Chemistry* **267**, 14551–14554.

Parker, I. & Ivorra, I. (1990). A slowly inactivating potassium current in native oocytes of *Xenopus laevis*. *Proceedings of the Royal Society* B **238**, 369–381.

Parker, I. & Miledi, R. (1988). A calcium-independent chloride current activated by hyperpolarization in *Xenopus* oocytes. *Proceedings of the Royal Society* B **233**, 191–199.

Peres, A. & Bernardini, G. (1983). A hyperpolarization-activated chloride current in *Xenopus laevis* oocytes under voltage-clamp. *Pflügers Archiv* **339**, 157–159.

Peres, A., Bernardini, G., Mancinelli, E. & Ferroni, A. (1985). A voltage-dependent K^+ channel controlling the membrane potential in frog oocytes. *Pflügers Archiv* **403**, 41–46.

Pusch, M. & Jentsch, T. J. (1994). Molecular physiology of voltage-gated chloride channels. *Physiological Reviews* **74**, 813–827.

Reid, J. D., Lukas, W., Shafaatian, R., Bertl, A., Scheurmann-Kettner, C. A., Guy, H. R. & North, R. A. (1996). The *S. cerevisiae* outwardly-rectifying potassium channel (DUK1) identifies a new family of channels with duplicated pore domains. *Receptors and Channels* (in the Press).

STUHMER, W., RUPPERSBERG, J. P., SCHROTER, K. H., SAKMANN, B., STOCKER, M., GLESE, K. P., PERSCHKE, A., BAUMANN, A. & PONGS, O. (1989). Molecular basis of functional diversity of voltage-gated potassium channels in mammalian brain. *EMBO Journal* **8**, 3235–3244.

TAGLIETTI, V., TANZI, F., ROMERO, R. & SIMONCINI, L. (1984). Maturation involves suppression of voltage-gated currents in frog oocyte. *Journal of Cellular Physiology* **121**, 576–588.

Acknowledgements

T.T. was on leave from the Kurume University while he was at the Glaxo Institute for Molecular Biology and was supported in part by a Grant-in-Aid for Exploratory Research from the Ministry of Education, Science, Sports and Culture of Japan.

Author's email address

T. Tokimasa: tokimasa@is.icc.u-tokai.ac.jp

Received 7 February 1996; accepted 19 July 1996.